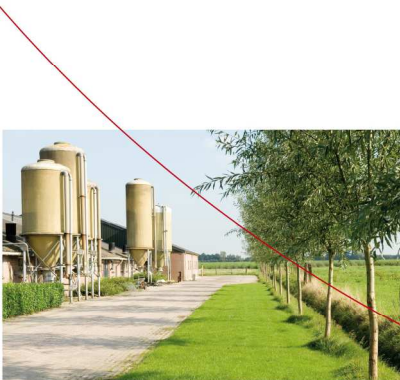




**Knowledge
for Climate**

WindVisions: First Phase Final Report





Copyright © 2012

National Research Programme Knowledge for Climate/Nationaal Onderzoekprogramma Kennis voor Klimaat (KvK) All rights reserved. Nothing in this publication may be copied, stored in automated databases or published without prior written consent of the National Research Programme Knowledge for Climate / Nationaal Onderzoekprogramma Kennis voor Klimaat. Pursuant to Article 15a of the Dutch Law on authorship, sections of this publication may be quoted on the understanding that a clear reference is made to this publication.

Liability

The National Research Programme Knowledge for Climate and the authors of this publication have exercised due caution in preparing this publication. However, it cannot be excluded that this publication may contain errors or is incomplete. Any use of the content of this publication is for the own responsibility of the user. The Foundation Knowledge for Climate (Stichting Kennis voor Klimaat), its organisation members, the authors of this publication and their organisations may not be held liable for any damages resulting from the use of this publication.

WindVisions: First Phase Final Report

WindVisions - an airport Wind and Visibility Monitoring System for critical weather conditions in a changing climate

Authors: Dr. Ir. O.K. Hartogensis, Ir. D. van Dinther and Prof. Dr. A.A.M. Holtslag



Wageningen University, Meteorology and Air Quality Group

CfK report number KfC 56/2012
ISBN EAN 978-94-90070-58-8

This research project (KvK HSMS01KfC 56/2012; WindVisions WindVisions: First Phase Final Report) was carried out in the framework of the Dutch National Research Programme Knowledge for Climate (www.knowledgeforclimate.org) This research programme is co-financed by the Ministry of Infrastructure and the Environment .



Content

Content.....	5
Summary	7
Samenvatting	9
1 Project Background.....	11
1.1 Problem Definition.....	11
1.2 Project Objective	13
1.3 Project Organization	14
2 Project Activities and Results.....	15
2.1 Scintillometer Development.....	15
2.1.1 Introduction.....	15
2.1.2 Method.....	16
2.1.3 Instrumentation.....	19
2.1.4 Experimental set-up	20
2.1.5 Results	21
2.1.6 Conclusions.....	25
2.2 SODAR development	27
2.2.1 Introduction.....	27
2.2.2 Instrumentation.....	28
2.2.3 Experimental set-up	29
2.2.4 Results	30
2.2.5 SODAR compared to LIDAR	35
2.2.6 Conclusions.....	36
3 Conclusions and Outlook	37
4 Literature	41





Summary

The operations at Mainport Schiphol are highly sensitive to a number of critical weather parameters, most notably precipitation, the local wind field and visibility. For save and efficient airport operation now and in the future, under the condition of a changing climate, routinely monitoring and prediction of these-critical weather parameters is essential.

It is the objective of this project to develop a Wind and Visibility Monitoring System (WindVisions) at Mainport Schiphol. WindVisions will consist of a crosswind scintillometer, which is a horizontal long range wind and visibility sensor, and a SODAR (Sound Detecting And Ranging), a vertical scanning wind sensor. The area of interest to monitor is the landing and take-off course of airplanes ranging from the surface to about 300m height along a runway.

This document reports on Phase 1 of WindVisions, which is characterized by the development and testing of the system. Phase 2 of WindVisions will be geared towards the operational implementation of the system at Schiphol Airport.

The main results from WindVisions Phase 1 are the development and testing of innovative cross-wind algorithms (calculation methods) for a single aperture scintillometer (SA-LAS) and testing of SFAS64 mini-SODAR of Scintec AG at the KNMI meteorological observatory of Cabauw. Regarding the cross-wind scintillometer work, we obtained the crosswind from a single aperture scintillometer (SA-LAS) signal using three different algorithms, which are based on scintillation power spectra without a calibration in the field. These algorithm are; the corner frequency (CF), maximum frequency (MF) and cumulative spectrum (CS). A field experiment was conducted at the Haarweg Meteorological Station in Wageningen, the Netherlands. All three algorithms obtained similar results for the scintillometer crosswind compared with a sonic anemometer, which was used as a reference. However, we conclude that the CS algorithm is best qualified to obtain crosswinds. First, because it is the algorithm with the best fit and lowest scatter in comparison to the sonic anemometer. Second, the results based on power spectra using Wavelets indicated that this method is well suited to obtain the crosswind over 1 second. The results of this study have been submitted the Journal of Atmospheric and Ocean Technology.

Regarding the SODAR work, the experiment at Cabauw revealed that the SODAR wind field measurements are comparable to that of the tower measurements. However, at some measurement heights (80 m) the agreement with the



tower is better than at other levels. In general the horizontal wind speed seems to be overestimated at greater heights (140 and 200 m). The wind direction compared very well to that of the tower. However, some scatter occurred in the wind direction measured by the SODAR for low wind speed. For the application for WindVisions this will not cause a problem, since low wind speeds do not introduce a safety risk for aircrafts landing or taking off. In all the SFAS64 SODAR performs well enough to proceed with this instrument as part of WindVisions.



Samenvatting

De activiteiten op Mainport Schiphol zijn met name gevoelig voor het lokale windveld en zicht. Gegeven de huidige en verwachte klimaatverandering zal deze gevoeligheid voor het lokale weer waarschijnlijk toenemen, aangezien extreme weergebeurtenissen naar verwachting frequenter en met een verhoogde intensiteit zullen optreden. Extreem weer betekent een veiligheidsrisico, maar ook economische verliezen als gevolg van extra vertragingen, omleidingen en vaker aan de grond blijven staan van vliegtuigen. Om haar positie als mainport te kunnen behouden, moet Schiphol zich aanpassen aan een veranderend klimaat om meer klimaatbestendig te worden.

Het doel van het onderzoek is de ontwikkeling van een Wind en Visibility Monitoring System (WindVisions) op Mainport Schiphol. Het systeem zal bestaan uit een horizontaal opererende lange-aftandsensor (een zogenaamde zijwind scintillometer) en een verticaal scannende sensor (een zogenaamde Sound detecting- and-ranging instrument: SODAR). Het gebied dat het systeem zal bemeten is de landing en take-off zone van vliegtuigen van het grondoppervlak tot 300m hoogte langs landingsbanen.

Dit rapport beschrijft de resultaten van Fase 1 van WindVisions, dat was gericht op het ontwikkelen en testen van het systeem. Fase 2 van WindVisions zal zich richten op de operationele toepassing van het systeem op Schiphol Airport.

De belangrijkste resultaten van Fase 1 van WindVisions zijn de ontwikkeling en het testen van innovatieve cross-wind algoritmes (rekenmethodes) voor een enkele-opening ofwel een single-aperture scintillometer (SA-LAS) en voor het testen van de SFAS64 mini-SODAR van Scintec AG bij het KNMI meteorologische observatorium van Cabauw. Voor de zijwind scintillometer ontwikkelden we drie verschillende algoritmes om de zijwind van een enkele opening scintillometer (SALAS) te verkrijgen op basis van scintillatie power spectra. Deze algoritmes zijn: de hoek-frequentie of corner-frequency (CF), maximale-frequentie (MF) en cumulatieve-spectrum (CS). De methodes zijn getest op basis van experiment dat is uitgevoerd op het meteorologisch meetstation Haarweg in Wageningen, Nederland. Alle drie de algoritmes gaven vergelijkbare resultaten voor de cross-wind in vergelijking met een sonische anemometer, die als referentie diende. Echter, we concluderen dat de CS-algoritme het beste algoritme is. Ten eerste, omdat het de algoritme met de beste fit en laagste spreiding is in het vergelijking met de sonische anemometer. Ten tweede tonen de resultaten op basis van power spectra uit Wavelets dat deze methode het beste is in bepalen van de zijwind over zeer korte intervallen, korter dan 1 seconde. De resultaten



van deze studie zijn vervat in een wetenschappelijk artikel dat is ingediend bij het Journal of Atmospheric and Ocean Technology.

Met betrekking tot het SODAR werk is uit het vergelijkingsexperiment op Cabauw gebleken dat de SODAR windveldmetingen goed overeenkomen met die van de mastmetingen. Echter, op sommige meethoogtes (80 m) zijn de overeenkomsten groter dan op andere hoogtes. In het algemeen lijkt de horizontale windsnelheid op grotere hoogten (140 en 200 m) met de SODAR metingen te worden overschat. De windrichting vergelijkt goed met de mast op alle hoogtes. Voor de lage windsnelheden is er wel meer spreiding waarneembaar. Voor de toepassing van WindVisions zal dit niet leiden tot een probleem, aangezien bij lage windsnelheden er geen veiligheidsrisico geldt voor vliegtuigen bij landen of opstijgen. Over het algemeen presenteert de SFAS64 SODAR goed genoeg om door te gaan met dit instrument als onderdeel van WindVisions.



1 Project Background

1.1 Problem Definition

Impacts of Climate Change on Airport Operations

The impact of climate change on airports is directly felt by the effects of future weather on the airport operations. The main problem is that we do not know at present how climate change affects the critical weather conditions (such as wind and visibility) at the airport. Given the current and anticipated climate change (e.g., KNMI, 2008), the sensitivity to local weather is expected to increase, as extreme weather events are expected to occur more frequently and with increased intensity. Airports will have to adapt to a changing climate to become more “climate proof”. As such it is urgent to start to develop a monitoring system of the critical weather elements.

When successful, WindVisions in continuous operation mode will allow swift adaptations in the operational plans to changes in local wind and visibility in the short run. For the longer run the detailed 3D wind-field and visibility measurements will record the local climate change at airports which will aid the strategic planning of the airport. The WindVisions project complements the project on “The impact of climate change on the critical weather conditions at Schiphol airport (HSMS03)” and also provides inputs for the local prediction system to be developed within the latter project as well as local observations for model evaluation.

For safety, cross- and tailwind values are restricted to certain limits. Depending on the condition of the runway, these limits are 20 kts for crosswind and 7 kts for tailwind. Sudden fluctuations in the wind (gusts) of 10 kts and more should be included in the total wind intensity. When crosswind limits are exceeded and there are less runways available which are parallel to the wind, this will lead to a loss of available operational airport capacity.

Another issue related to wind near the runway is the wake vortex generated behind airplanes. The wake vortex is the turbulent spiralling wind of the wing-tips of airplanes. These type of flows can overturn small aircraft and dangerously disturb the course of larger airplanes.

Adverse visibility conditions have a direct negative influence on the available operational capacity. For example, at Schiphol airport the number of arrivals



and departures reduces by a factor 2 when visibility is less than 600 m or when cloud ceiling is less than 200 ft. Accurate monitoring of these conditions will allow for a more efficient use of the available airport capacity. Apart from airport capacity it is evident that adverse wind and visibility conditions compromise the safety of airport operations. A detailed local monitoring system of wind and visibility allows a quick reaction to changes in local weather.

The knowledge developed within this project is for airports in general and may be applicable to other transport infra-structures as well. Our initial focus will be on Mainport Schiphol. Specific for the situation at Schiphol Mainport is that the dominant wind-direction is presently South-West to West. For safety and efficiency, airplanes should maximize their possibility to land and take-off against the wind. Conflicting with this principle and the dominant wind direction is the fact that three of the five runways at Schiphol have a North-South orientation. In practice, therefore airplanes often operate under crosswind and sometimes tailwind conditions.

The Problem

The operations at airports are in particular sensitive to the local wind field and visibility. For save and efficient airport operation now and in the future under the condition of a changing climate routinely monitoring of the 3D-windfield and visibility is essential. Currently wind measurements and visibility measurements are taken at one or just a few locations over an airport. The equipment used is standard for meteorological stations. Especially the distribution and the type of wind sensors (cup anemometers) are not adequate to monitor the wind-field in the area of interest, the so-called approach and touchdown-zone. The approach zone encompasses the air-space in front of the runway where planes are in the last 300 m of their approach (or conversely their take off). The touchdown zone represents the first or last 30% of the runway.

As climate change is happening right now it is important to quickly start building up a homogenous and detailed data-set with which the impact of local climate change at airports on wind and visibility can be monitored. Such a data-set will aid strategic the planning of airports, and other transport infra-structures, in the future and keep them climate-proof. Apart from adaptations in the long-term planning for which we first need to gather a comprehensive data-set some of the adaptations to climate change can be made in the short-term, such as change in the operational plans and usage of runways.

In addition, it will also aid local weather forecasting in particular for circumstances with extreme weather. In the short run this should reduce errors in existing, incomplete measurements and as such increase the safety and efficiency of the day to day airport operations.



1.2 Project Objective

The objective of this project is to develop a Wind and Visibility Monitoring System (WindVisions) at airports. The system will consist of a by a horizontal long range wind sensor, a so-called cross-wind scintillometer complemented by a vertically scanning remote sensing instrument, a so-called sound detecting and ranging instrument (SODAR). The area of interest to monitor is the landing and take-off course of airplanes ranging from the surface to about 300m height along a runway (see Figure 1).

13

As we focus on wind and visibility data that support the landing phase of aircraft, the scintillometer and SODAR types are chosen reflect that objective. In the vertical a mini-SODAR will be used that gives information on averaged wind speed with a high vertical resolution of 5m up to a height of ~250m. Along the runway the scintillometer provides a path averaged cross-wind and visibility at a height of choice ranging between 2 to 20m. The scintillometer should not be seen as a replacement of traditional instrumentation already used at airports, but rather as a complimentary path averaged measure of the cross-wind.

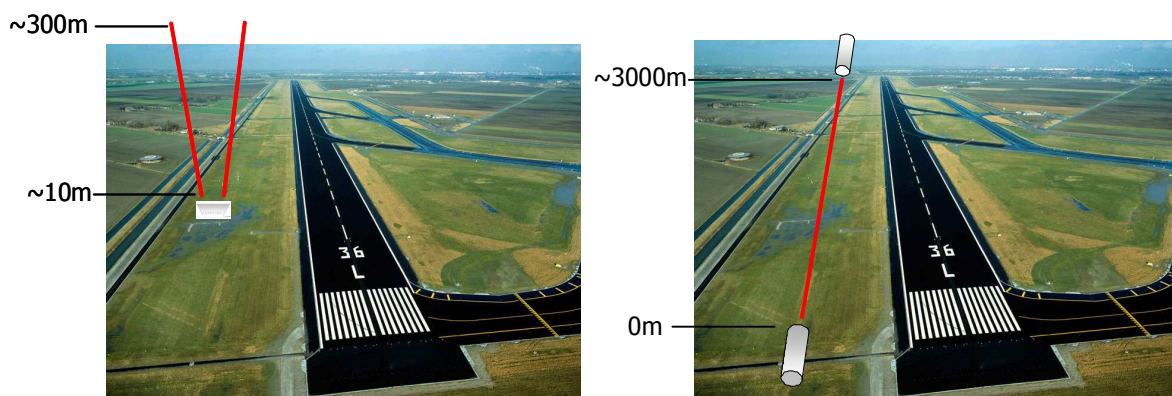


Figure 1: SODAR measures the wind field vertically from 10 up to 300 m (left), while a scintillometer obtains a path averaged crosswind with a path length ranging from 100 m to a few kilometres (right).

The research will be divided in two phases. The first phase deals with the proof of concept of the system and the second phase will be geared towards implication of WindVisions into the operational practice at Schiphol airport. Currently we report on phase 1, in which we developed and tested a WindVisions prototype based on a cross-wind scintillometer and SODAR. We will also shortly comment on the suitability of SODAR versus LIDAR (light detection and ranging) systems to form part of WindVisions.



1.3 Project Organization

This study is organized as a four year PhD-project. For funding reasons the project is divided over two Phases following the organization of the Knowledge for Climate Program (Kennis voor Klimaat - KvK) issued by the Dutch government:

Phase 1:

KvK is organized by Hotspots in Phase1 of which MainPort Schiphol is one. WindVisions in Phase1 will focus mainly on the technological development of WindVisions. Development will mainly take place in Wageningen and the KNMI observatory in Cabauw.

- Technology Development
- Location: Mainly in Wageningen and Cabauw
- Time: 2010 – 2012
- Deliverables:
 - Prototype of WindVisions
 - Testing phase in Wageningen and Cabauw
 - Novel instrument development on cross wind scintillometry:
 - Improved algorithms for the double-receiver scintillometer.
 - Fully working proto-type of a single receiver scintillometer fitted with a striped-filter.
 - Horizontal and vertical wind measurements (down-drafts)

Phase 2:

KvK is organized by Themes in Phase2. WindVisions is part of Theme 6 (Climate Projections). WindVisions in Phase2 will focus on the deployment of WindVisions at Schiphol. Development will mainly take place in Wageningen and the KNMI observatory in Cabauw.

- Deployment WindVisions
- Location: Mainly at Schiphol
- Time: 2012 – 2014
- Deliverables:
 - Operational WindVisions System at Schiphol Airport
 - Synergy/Embedment with IMPACT to come to one measurement and forecast package for wind and visibility at Schiphol Mainport
 - HARMONIE Model output delivered by IMPACT will be confronted with the observations by WindVisions.
 - PhD thesis

The project is currently in its second phase. This report covers an overview of the work done in phase 1. It should be noted that this *final* report of Phase 1 is somewhat artificial as we are in the middle of an on-going PhD project.



2 Project Activities and Results

2.1 Scintillometer Development

The scintillometer work in the first phase of WindVisions focused on obtaining the crosswind from a Single-Aperture Large-Aperture-Scintillometer scintillometer (SA-LAS). This work is described in a scientific article entitled 'Crosswind from a Single Aperture Scintillometer using Spectral Techniques' submitted to the *Journal of Atmospheric and Oceanic Technology* (Van Dinther et al., 2012). The main findings are discussed below.

2.1.1 Introduction

A scintillometer is a device that consists of a transmitter and receiver. The transmitter and receiver are placed over a path of 0.1 to 10 km. The transmitter emits a light beam which is refracted in the turbulent atmosphere, causing light intensity fluctuations that are measured by the receiver. The scintillometer is best known for measuring area averaged surface fluxes (among others Meijninger et al. 2002a, Meijninger et al. 2002b, Green et al. 2001, and Beyrich et al. 2002), but it can also obtain the path averaged wind component perpendicular on a path, the so called crosswind (U_{\perp}).

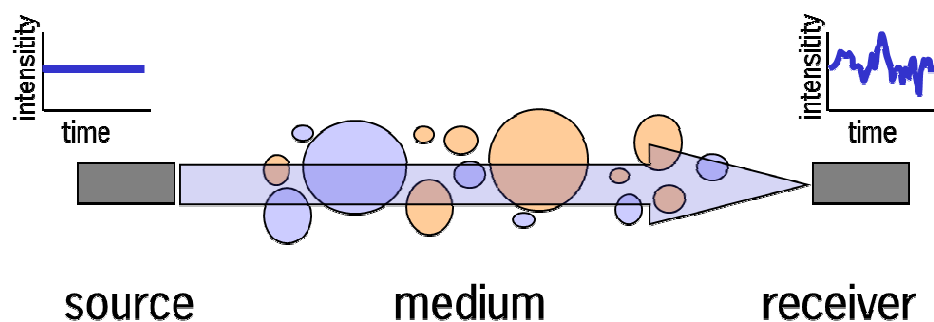


Figure 2: Schematic of a scintillometer; the source or transmitter emits a light beam with constant intensity, at the receiver the light intensity fluctuates as a result of turbulent air.

An application of line averaged crosswinds obtained from scintillometers is at airports. Strong crosswind along airport runways can introduce a serious safety risk to airplanes taking off or landing. Therefore, take-off and landing at air-



ports are restricted to a crosswind limit of 20 knots (10 m s⁻¹). Wong et al. (2006) showed that above 18 knots (9 m s⁻¹) the "relative accident involvement ratio" at airports is much higher than for crosswinds below 18 knots (around 6.5 compared to 1 for crosswind below 18 knots). When crosswind limitations are exceeded this will lead to a loss of available operational capacity of the airport. Airports typically use cup anemometers and wind vanes to measure the crosswind. The disadvantage of these devices is that their measurements are representative for a small part of the runway, while the scintillometer averages the crosswind along a path. The along a line averaging of a scintillometer also makes it suitable to measure valley winds (Furger et al. 2001). Clifford (1971) developed a theoretical model for the scintillation power spectrum. In this model the crosswind over the scintillometer path determines its position along the frequency axis of the spectrum. Nieveen et al. (1998) used the theoretical scintillation spectra of Clifford (1971) to distinguish absorption from refraction fluctuations in the scintillometer signal. They noted that a salient frequency point in the spectrum, in their case the upper corner frequency, scales linearly with the crosswind. Therefore, by obtaining the frequency corresponding to a salient point the crosswind can be obtained.

2.1.2 Method

We use three different algorithms to determine the crosswind from the scintillation spectra. The algorithms are named after the salient points in different representation in the spectra, notably: the Corner Frequency (CF), Maximum Frequency (MF), and Cumulative Spectrum (CS) algorithm. The salient points shift linearly along the frequency axis as a function of U_{\perp} . Therefore, U_{\perp} can be determined using:

$$U_{\perp} = C_{algorithm} D f_{algorithm} \quad (1)$$

where $C_{algorithm}$ is a constant depending on the algorithm used, D is the aperture diameter of the scintillometer used, and $f_{algorithm}$ is the frequency corresponding to the salient points of the different algorithms. A new aspect in our approach is that the values of $C_{algorithm}$ will be determined from the theoretical model for the scintillation spectrum of Clifford (1971), instead of relying on experimental calibration.

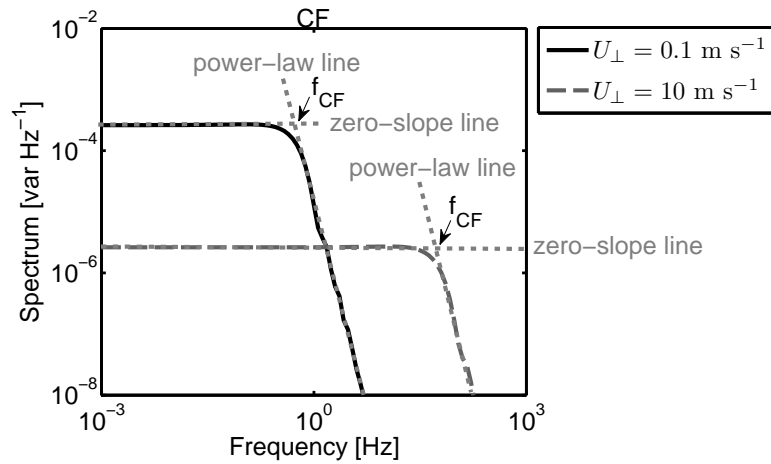


Figure 3: Theoretical scintillation spectra with a crosswind of 0.1 m s^{-1} (solid black line) and 10 m s^{-1} (dashed grey line) in loglog representation.

The CF algorithm is similar to the upper corner frequency described by Nieveen *et al.* (1998). The corner frequency is the inflection point in the loglog representation of the scintillation spectrum. We define it as the point of intersect between the zero-slope line and the power-law line (see Figure 3). The constant C_{CF} , describing the relation between the corner frequency and crosswind following Equation 1, is determined from the theoretical model and is 1.38.

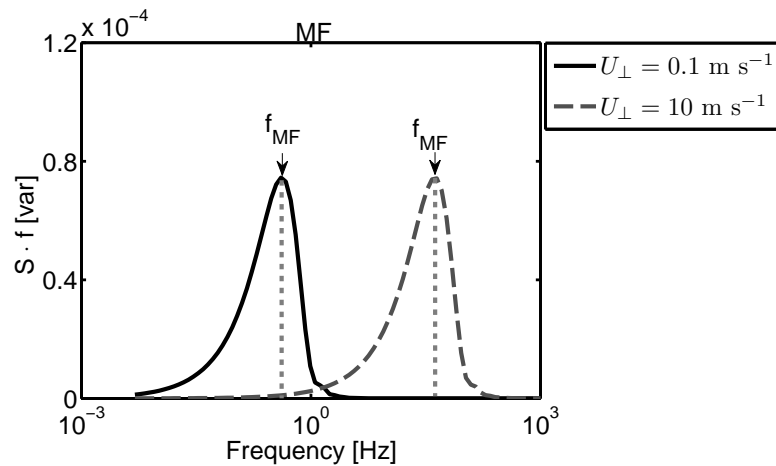


Figure 4: Theoretical energy conserved representation of the scintillation spectra with a crosswind of 0.1 m s^{-1} (solid black) and 10 m s^{-1} (dashed grey).

The MF algorithm is similar to the Fast Fourier Transform (FFT) technique described in Poggio *et al.* (2000). The maximum frequency (f_{MF}) is the frequency where the maximum of the energy conserved representation of the scintillation spectrum is located (see Figure 4). The constant C_{MF} in Equation 1, obtained from the theoretical model, is 1.59. This value is similar to the 1.63 value found by Ward *et al.* (2011).

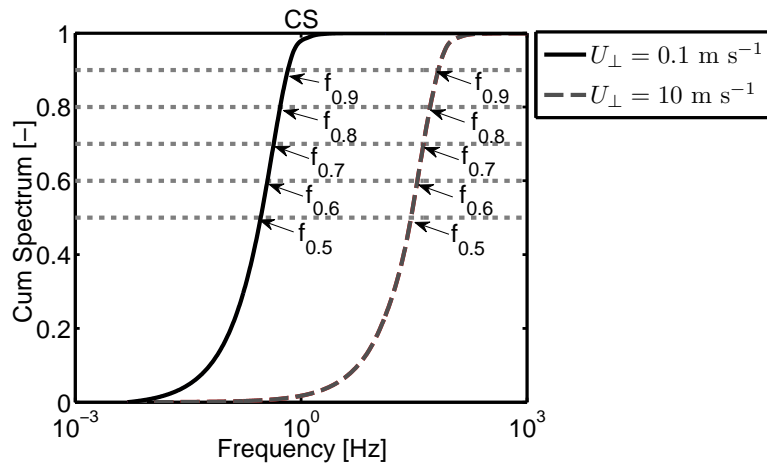


Figure 5: Theoretical cumulative scintillation spectra with a crosswind of 0.1 m s^{-1} (solid black line) and 10 m s^{-1} (dashed grey line).

The CS algorithm is a new technique to obtain the crosswind from scintillation spectra and uses the cumulative spectrum. This spectrum, also known as Ogives (Oncley *et al.* 1996), is obtained by integrating a spectrum from high to low frequencies. However, we integrate the spectrum from low to high frequency (left to right) and normalize the spectra with the variance ($\sigma_{ln(I)}^2$). Unlike the previously discussed algorithms, the CS algorithm takes into account the complete shape of the spectrum. We used five frequency points, which corresponded to the following points in the cumulative spectrum; 0.5, 0.6, 0.7, 0.8, and 0.9 (see Figure 5). The constants C_{CS} obtained from the theoretical spectra corresponding to these frequency points are 2.31, 1.88, 1.55, 1.27, and 1.00 respectively. The crosswinds obtained from these five points are averaged to obtain one crosswind per scintillation spectrum.

The scintillation spectra can be obtained from the scintillometer signal intensity measurements using Fast Fourier Transformation (FFT). However, with FFT we need at least 5 minutes of data to represent the scintillation spectrum well enough to determine the crosswind from the spectrum. To obtain the crosswind from scintillation spectra for shorter time intervals (≤ 1 minute) we will use spectra calculated with wavelets.

The algorithms described above all use the scintillation spectra. Therefore, errors can occur in the crosswind if the scintillation spectra are not obtained correctly. The spectra can be influenced by; unwanted contributions to the spectra, a low signal or signal to noise ratio, and variability of U_{\perp} along the path. The algorithms have different sensitivities for these phenomena's. Therefore, different filters were applied for the algorithms. A filter on signal intensity (I) was applied for all three algorithms, so data were I was below 20 000 arbitrary units were excluded. A high-pass filter (HPF) of 0.1 Hz was applied for the CF and MF algorithm. A low-pass filter (LPF) of 90 Hz was also applied on the MF algo-



rithm. For the CS algorithm data where the maximum frequency was below 0.1 Hz or above 0.9 Hz were also filtered out. Additionally, we tested a filter of $U_{\perp CS}$ below 0.5 m s^{-1} for the CS algorithm.

2.1.3 Instrumentation

As part of this project we purchased a BLS900 type Boundary Layer Scintillometer by Manufacturer Scintec in Rottenburg, Germany (see Figure 6). It consists of a dual aperture transmitter and a single aperture receiver, which can separate the two transmitted signals. The wavelength at which the BLS900 is operated is 880nm and the aperture diameter is 15cm, which makes it a Large Aperture Scintillometer (LAS). In all, the BLS900 is a dual-aperture LAS (DA-LAS).



Figure 6: BLS900 scintillometer consisting of a dual aperture transmitter and a single aperture receiver.

The processing units fitted with a mini-pc to facilitate raw data (500 Hz measurement frequency) storage have been built into a portable container for prolonged experiments under harsh weather conditions (see Figure 7). With the instrument thus prepared we are ready for the field tests at Schiphol Airport later on in the project.



Figure 7: Processing unit and mini-pc built into a weather proof case. The portable screen and keyboard are only connected when accessing the unit in the field.



2.1.4 Experimental set-up

The data studied here were collected at the meteorological site at the Haarweg, Wageningen, The Netherlands from 14 April till 20 May 2010. We deployed a Boundary Layer Scintillometer (BLS900, Manufacturer Scintec, Rottentburg, Germany). The BLS900 was installed at a height of 3.53 with a path length of 426 m (see Figure 8). The scintillometer is fitted with a processing unit that has a measurement frequency of 500 Hz. We stored the raw 500 Hz intensity signal. We used the Srun software version 1.07 of Scintec to operate the scintillometer. Even though the BLS900 is a DA-LAS, we will use only one of the two signals in our study. So in our analysis it effectively becomes a single-aperture LAS (SA-LAS). We will shortly discuss the results of the crosswind given by Srun, which uses an unspecified dual aperture scintillometer (DA-LAS) algorithm from the manufacturer.

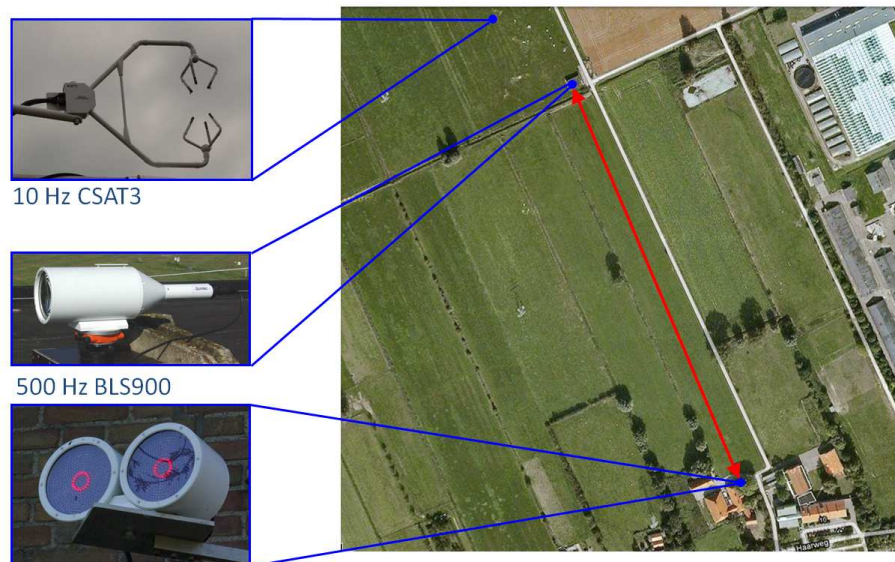


Figure 8: Overview of the location of the CSAT3 sonic anemometer and the BLS900 deployed at the Haarweg, Wageningen, the Netherlands. As a reference to the scale: the BLS900 path length (red arrow) is 426m.

The output of the BLS900 was validated against a CSAT3 sonic anemometer manufactured by Campbell scientific (Utah, United States of America), which was also located at the meteorological site at the Haarweg (see Figure 8). The sonic anemometer was not located in the scintillometer path, but at a distance of roughly 200 m. Assuming a homogeneous wind field this should not result in a substantial difference in wind speeds measured by the BLS900 and CSAT3, given the short distance between scintillometer and sonic anemometer and relatively short scintillometer path. The measurement height of the CSAT3 was 3.44 m. The measurement frequency of the sonic anemometer was 10 Hz. The wind components of the CSAT3 we used to calculate the crosswind were



aligned with the flow using a planar fit correction (Wilczak *et al.* 2001). To validate the BLS900 with the CSAT3, the wind component perpendicular to the scintillometer path was calculated from the horizontal wind components measured by the CSAT3.

We analysed the data measured from 13 till 19 May 2010 (DOY 133 until 139). In Figure 9 the wind measurements (speed and direction) of the sonic anemometer are plotted for these days. In stable conditions during night time the 2 m wind speed was suppressed and therefore relatively low (in general $< 2 \text{ m s}^{-1}$). In unstable conditions during day time the wind speed is in general higher with a maximum of 7 m s^{-1} on DOY 136. The wind direction during the measurement period was variable, but mainly from North / Northwest, which is unfortunately not very perpendicular to the scintillometer path.

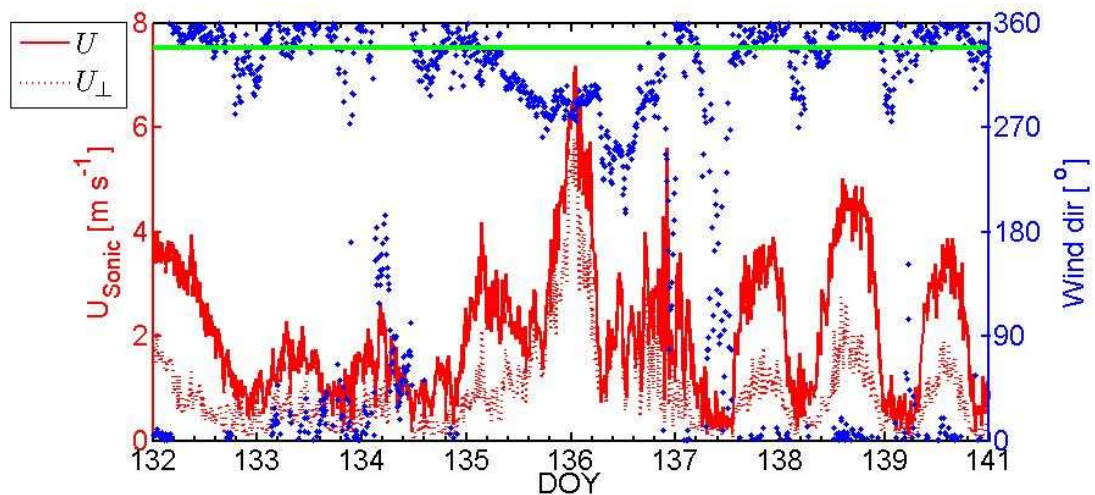


Figure 9: Wind conditions at the Haarweg from DOY 133 till 140, with horizontal wind speed (red solid line) and crosswind on the scintillometer path (red dashed line) on the left y-axis, and wind direction (blue dots) on the right y-axis. The orientation of the scintillometer path is given by the green line.

2.1.5 Results

In Figure 10, scatter plots are given of the crosswind measured by the sonic anemometer ($U_{\perp \text{Sonic}}$) against crosswind determined with the BLS900 (used as a SA-LAS - $U_{\perp \text{SA-LAS}}$) for the three algorithms obtained from FFT spectra over 10 minutes time intervals. The points are colour coded with the signal to noise ratio (SNR). By signal we here refer to the amount of light intensity fluctuations caused by scintillation, which is given by the standard deviation of the received light intensity. The noise level was determined in the field as the standard deviation of the light intensity measured by the receiver when the light intensity emitted by the transmitter was not received, which was 15 arbitrary units.



Table 1: Regression equations, R^2 and RMSE for $U_{\perp SA-LAS}$ with $U_{\perp Sonic}$ for CF, MF, and CS algorithm with different filters.

Algorithm	Filter	Regression eq.	R^2	RMSE	N [%]
CF	HPF	$y = 0.95x + 0.23$	0.81	0.46	80
MF	HPF & LPF	$y = 0.83x + 0.14$	0.70	0.53	83
CS	$0.1 > f_{MF} > 90$	$y = 0.95x + 0.22$	0.87	0.37	75
	$U_{\perp CS} < 0.5$	$y = 0.93x + 0.26$	0.85	0.39	64

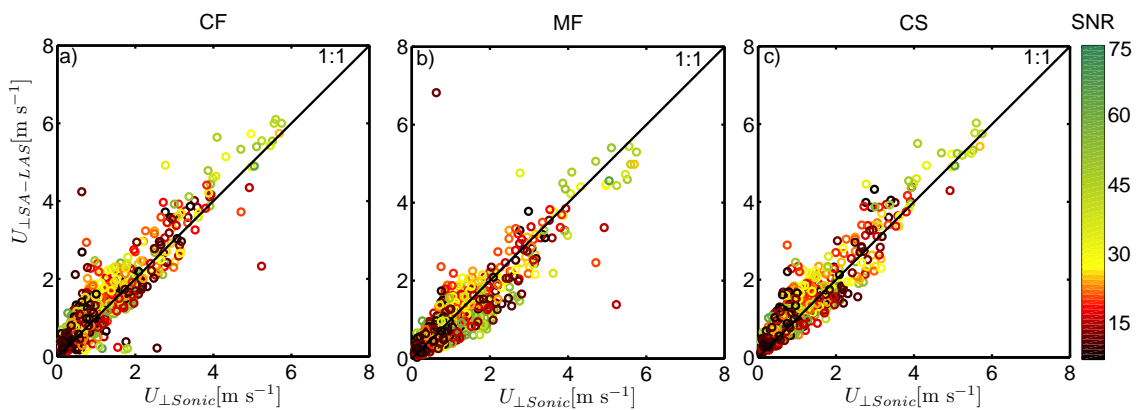


Figure 10: Scatter plots of 10 minute crosswinds averages of $U_{\perp Sonic}$ against $U_{\perp SA-LAS}$ for CF (a), MF (b) and CS (c) algorithm colour coded with SNR.

Figure 10 indicates that all spectral techniques obtained similar results as the $U_{\perp Sonic}$. This similarity between the spectral techniques and the sonic anemometer is also visible in the regression statistics outlined in Table 1. In this Table the linear regression parameter and corresponding R^2 , root mean square error (RMSE), and the percentage of data points left after filtering (N) are shown. Results of an additional HPF for the CF algorithm, and an additional filter on $U_{\perp CS} < 0.5$ for the CS algorithm are also shown. It should be noted that filtering on $I < 20\,000$ already resulted in a loss of data of 17 %. This high percentage is mainly caused by fog in the morning during this particular measurement period. The fit of $U_{\perp CS}$ with $U_{\perp Sonic}$ is best, with a regression slope of 0.95 and a RMSE of 0.37 $m\ s^{-1}$. However, the amount of data points is smallest for this algorithm, with a N of only 75 %. For the CF algorithm the fit with the sonic anemometer is also very good (with a regression slope of 0.95). However, the scatter is somewhat higher than that of the CS algorithm (R^2 of 0.81 in comparison to 0.87, and a RMSE of 0.46 in comparison to 0.37). We assumed that the CS algorithm would not be valid for crosswinds below 0.5 $m\ s^{-1}$. However, using a filter on these low crosswinds did not improve the results, but did result in an extra loss of data of 11 %. The fit of the MF algorithm with the sonic anemometer is worst of the three spectral techniques (regression slope of 0.83 and RMSE of 0.53 $m\ s^{-1}$). On the other hand all the data points, where the signal intensity is not below



20000, result in a value for the crosswind. Therefore, the MF algorithm is most robust in determining the crosswind. From Figure 10b it is apparent that some outliers in U_{MF} occur when the SNR is low (< 10).

As previously mentioned, the crosswind can be calculated using wavelets for every second. For this analysis we used data of one day only, which was 16 May 2010 (DOY 136). To compare the crosswinds for every second does not make any sense, since the clocks of the BLS900 and sonic anemometer were not synchronized to the second and the location of the two instruments was not the same. Therefore, in order to validate the BLS900 with the sonic anemometer crosswinds obtained from 1 second wavelet spectra were averaged over 10 minutes. At least 70 % of the 1 second data had to be present to average over 10 minutes.

Table 2: Regression equations, R^2 and RMSE for $U_{\perp SA-LAS}$ with $U_{\perp Sonic}$ for CF, MF, and CS algorithm with wavelets for DOY 136.

Comparison	Algorithm	Regression eq.	R^2	RMSE	N [%]
$U_{\perp SA-LAS}$ vs $U_{\perp Sonic}$	CF	$y = 0.97x + 0.58$	0.88	0.46	78
	MF	$y = 0.89x + 0.12$	0.89	0.41	100
	CS	$y = 1.06x + 0.37$	0.89	0.47	100
$STD_{U_{\perp SA-LAS}}$ vs $STD_{U_{\perp Sonic}}$	CF	$y = 0.82x + 0.30$	0.87	0.11	78
	MF	$y = 0.96x + 0.30$	0.88	0.13	100
	CS	$y = 0.58x + 0.17$	0.82	0.10	100

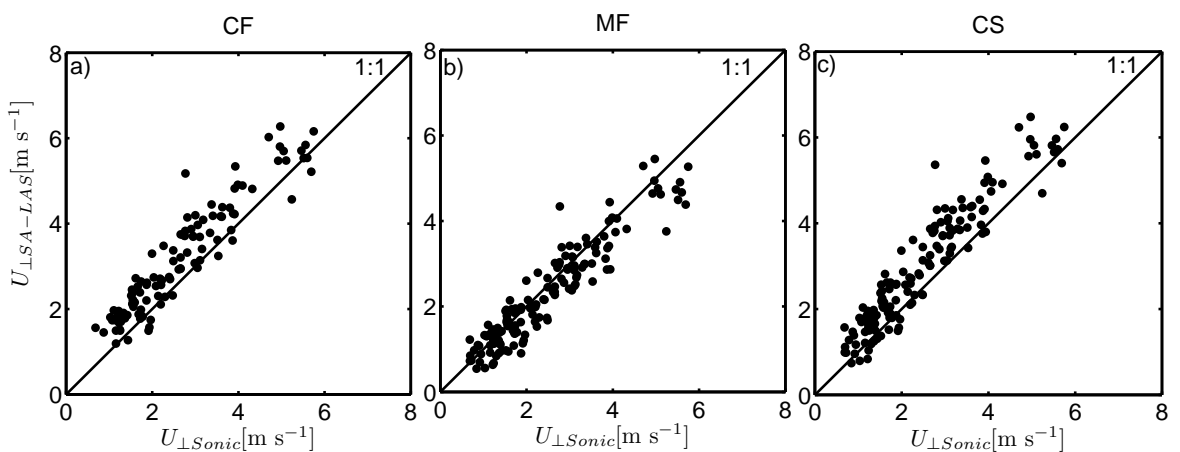


Figure 11: Scatter plots of 10 minute crosswinds averages obtained from 1 second wavelets with on the x-axis $U_{\perp Sonic}$ and on the y-axis $U_{\perp SA-LAS}$ for CF (a), MF (b), and CS (c) algorithm, on DOY 136.

Results of crosswind using the wavelet technique for DOY 136 are plotted in Figure 11, and regression statistics are shown in Table 2. From this Figure and



Table we conclude that the three algorithms all compare well to $U_{\perp\text{Sonic}}$ when wavelets are used. The scatter is low for all the algorithms with R^2 -values of 0.88 and 0.89, and the RMSE range from 0.41 to 0.47.

Even though it does not make sense to compare $U_{\perp\text{SA-LAS}}$ with $U_{\perp\text{Sonic}}$ for every second, the 1 second crosswinds enable us to calculate the standard deviation for every 10 minute interval which can be compared with each other. It is important to note here that the SA-LAS measures a path averaged crosswind, while the wind of the sonic anemometer is a point measurement. We therefore expect the standard deviation of $U_{\perp\text{SA-LAS}}$ to be lower than that of $U_{\perp\text{Sonic}}$, since crosswind extremes are already averaged out by a SA-LAS because of its path weighting.

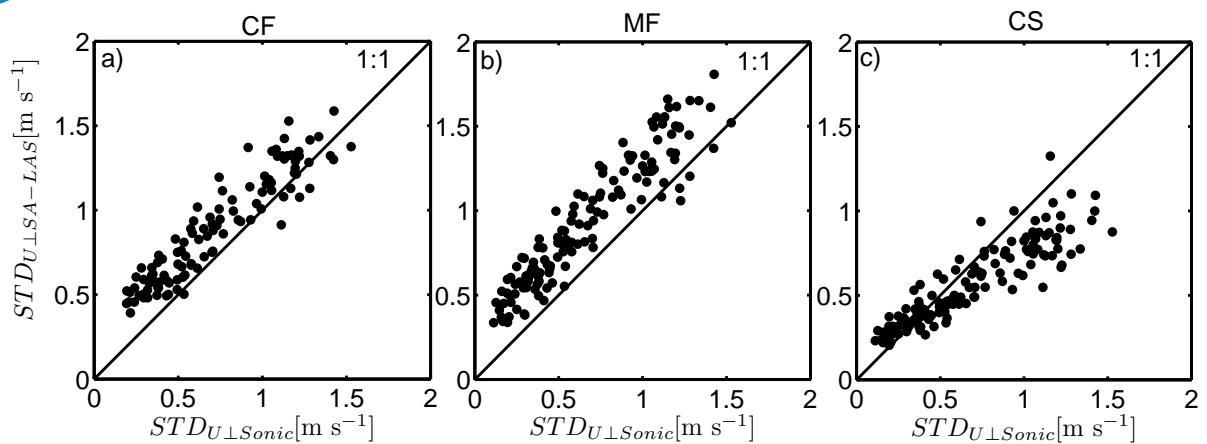


Figure 12: Scatter plots of 10 minute standard deviations from 1 second crosswinds from wavelets with on the x-axis $STD_{U_{\perp}\text{Sonic}}$ and on the y-axis $STD_{U_{\perp}\text{SA-LAS}}$ for CF (a), MF (b), and CS (c) algorithm for DOY 136.

We present the results for the 10 minute standard deviation in Figure 12 and the regression statistics are shown in Table 2. Unexpectedly, the standard deviation for the CF and MF algorithm are even somewhat overestimated compared to the standard deviation of $U_{\perp\text{Sonic}}$. For the MF algorithm, this is probably caused by the fact that this method takes into account only one point in the spectrum. Only considering one point can introduce extra noise when the location of this point is not well defined, resulting in a larger $STD_{U_{\perp}\text{MF}}$. The CF algorithm takes into account multiple points in the spectrum, since the corner frequency is determined from the zero-slope line and power-law line. The zero-slope line is located at low frequencies, and the power-law line is located at high frequencies. Therefore, the power-law line can fluctuate for the different 1 second spectra, while the zero-slope line is more fixed, which can cause the overestimation of $STD_{U_{\perp}\text{CF}}$. The CS algorithm takes into account the whole shape of the spectrum. The standard deviations of the crosswind of this algorithm are, as expected, lower than that of the sonic. This lower standard deviation



enhances our confidence in this algorithm to obtain the crosswind over short averaging times using wavelets.

Scintec also implemented an algorithm to obtain the crosswind. However, which algorithm they use is unknown. They use a DA-LAS approach, which has the advantage that the sign of the crosswind is known. The 10 minute results of this DA-LAS approach are plotted against $U_{\perp\text{Sonic}}$ in Figure 13, without (a) and with (b) a filter on $I < 20\,000$. $U_{\perp\text{DA-LAS}}$ overestimates $U_{\perp\text{Sonic}}$ considerably (regression slope of 1.19). The scatter of $U_{\perp\text{DA-LAS}}$ with $U_{\perp\text{Sonic}}$ is slightly higher than that of $U_{\perp\text{SA-LAS}}$ of our three algorithms. Although the fit is not very good of Scintec's algorithm with the sonic, the amount of data points is higher for their algorithm than the spectral techniques. Apparently, Scintec's algorithm is able to obtain the crosswind also when the scintillometer signal is low, albeit not the correct value of U_{\perp} . Applying a filter on $I < 20\,000$ did not improve the results of Scintec's algorithm.

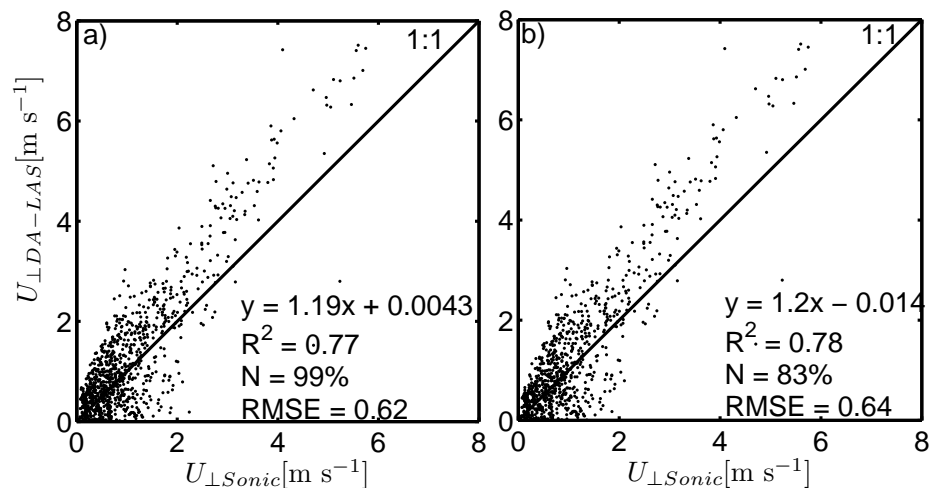


Figure 13: Scatter plots of 10 minute crosswinds averages with on the x-axis $U_{\perp\text{Sonic}}$ and on the y-axis $U_{\perp\text{DA-LAS}}$ of Scintec's algorithm without any filtering (a) and with a filter on $I < 20\,000$ (b).

2.1.6 Conclusions

We obtained the crosswind from a single aperture scintillometer (SA-LAS) signal using three different algorithms, which are based on scintillation spectra without a calibration in the field. These algorithm are; the corner frequency (CF), maximum frequency (MF) and cumulative spectrum (CS). All three algorithms obtained similar results for the crosswind compared with a sonic anemometer, thereby proving that the three algorithms are able to obtain the crosswind from a scintillometer signal. However, some filters needed to be ap-



plied to obtain these results. A filter on the scintillometer intensity signal (I) was applied to all algorithms ($I < 20\,000$).

The CF algorithm has the disadvantage that it does not yield a result when the zero-slope and power-law line are not clearly present in the scintillometer spectrum. On the other hand this does serve as a quality check for how well the spectrum of the scintillometer signal is defined. This built in quality check is why this method achieves good results, also without additional filtering. Applying a high-pass filter did improve the results of the CF algorithm.

The MF algorithm was most robust in obtaining the crosswind, only an additional high-pass filter and low-pass filter were applied. These filters did not result in a loss of data. For the MF algorithm it was also possible to use a less strict filter on signal intensity (5 000 instead of 20 000) and still achieve similar results for the regression statistics as with the strict filter. In this study we also discussed a signal to noise filter, but in the end we did not apply this filter to our data.

The CS algorithm, a new algorithm we introduced in this paper, achieved the best result. The root mean square error was smallest for this algorithm (0.37 compared to 0.46 and 0.53). Also the scatter of $U_{\perp CS}$ with $U_{\perp Sonic}$ was smallest, with R^2 of 0.87 compared to 0.81 and 0.70. On the other hand, the amount of data points of the CS algorithm was smallest, since all the data points where the maximum frequency was below 0.1 Hz or above 90 Hz were filtered out. For short time intervals (≤ 1 minute) we recommend using wavelets in combination with the CS algorithm. The ten minute average of crosswinds obtained from wavelet spectra averaged over 1 second showed similar results as the sonic anemometer. We expected the 10 minute standard deviations of the crosswind of the SA-LAS to be lower than that of the sonic anemometer, since the scintillometer levels out the extremes due to its path averaging. For the CS algorithm this expectation held, with a regression slope of 0.58. However, the standard deviations of the CF and MF algorithm were similar to that of the sonic anemometer (regression slopes of 0.82 and 0.96). Probable cause for the MF algorithm is that it only uses one point, which can introduce extra noise, and thereby lead to a higher standard deviation. For the CF algorithm the high standard deviation of the crosswind is probably caused by strong variation in the location of the power-law line probably caused by fluctuations in the structure parameter of the refractive index.

From the results we obtained, we conclude that the CS algorithm is best qualified to obtain crosswinds. First, because it is the algorithm with the best fit and lowest scatter with the sonic anemometer. Second, the results of the wavelet spectra also indicated that this method is best suited to obtain the crosswind over 1 second.

In this study we used the BLS900, a commercial dual aperture scintillometer (DA-LAS) manufactured by Scintec (Rottenburg, Germany), which for our analysis we treated as a single aperture scintillometer (SA-LAS). The Scintec's Srun software (version 1.07) provides a crosswind estimate using an undocumented



DA-LAS approach. The crosswind obtained from the Srun algorithm showed a clear overestimation of approximately 20 %. Also the scatter of $U_{\perp\text{DA-LAS}}$ with $U_{\perp\text{Sonic}}$ was higher than that of $U_{\perp\text{SA-LAS}}$ with $U_{\perp\text{Sonic}}$. These results imply that our spectral techniques achieve better crosswind results than that of Scintec's Srun algorithm. A disadvantage of the spectral techniques is that the sign of the crosswind is not known. We suggest using the value of the crosswind of a spectral technique in combination with the sign information from a DA-LAS algorithm.

For WindVisions the wind measurements ideally have to be available in real time. This can be achieved by using a measurement card which continuously computes FFT spectra. However, for the lower frequencies the longer time-scales will determine the height of the scintillation power spectrum. Therefore, it is advisable to use a SA-LAS algorithm where the salient point in the spectrum is located at higher frequencies. For the CS algorithm this is the case, especially for the 0.9 point in the cumulative spectrum. Future research will therefore focus on obtaining the crosswind real time using the CS algorithm.

2.2 SODAR development

2.2.1 Introduction

A sound detecting and ranging (SODAR) instrument is a vertically scanning remote sensing instrument. A SODAR obtains the wind speed and direction at different heights, and also provides information about the characteristics and structure of the boundary layer turbulence. A SODAR emits sound waves, which are backscattered by temperature inhomogeneities in the atmosphere. These temperature inhomogeneities move with the wind. Therefore, the wind speed can be determined from the Doppler frequency shift observed in the backscattered signal (see Figure 14). By emitting sound waves in three different directions the 3D wind field can be obtained.

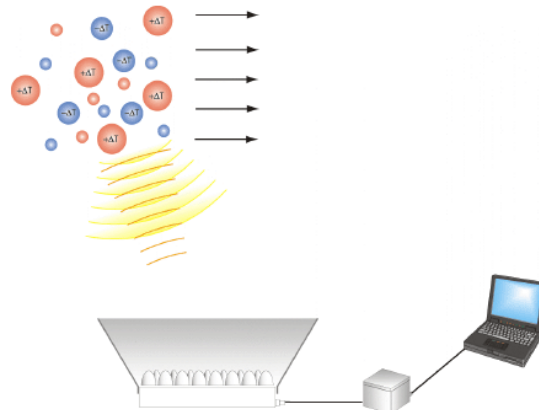


Figure 14: Schematic of a SODAR. The instrument emits a sound pulse which is reflected back by turbulent eddies in the atmosphere. The reflected sound pulse exhibit a Doppler shift as the eddies are moved along with the prevailing wind.

2.2.2 Instrumentation

The SODAR used in this study is a small flat array antenna SODAR (type SFAS64) manufactured by Scintec in Rottenburg, Germany (see). The SFAS64 is a compact SODAR, which has a relatively short vertical range with a high vertical resolution of up to 5 m. This makes the SODAR suitable for WindVisions. This SODAR has two tilt angles over which the sound can be emitted; 19° and 24°. The 19° tilt angle is recommendable for sites with ground clutter. However, a smaller tilt angle may result in a stronger variability of the horizontal wind measurements. It is a multi-frequency SODAR, which allows an optimal range (low frequencies yield largest range but with limited resolution) with optimal resolution where it is needed most, i.e. in the lowest levels (high frequencies yield highest resolution but with limited range)



Figure 15: SFAS64 flat antenna array SODAR by Scintec consisting of 64 piezo-electric transducers (sound emitting and receiving units).



The SODAR we use in this project is owned by the Meteorology and Air Quality group. During this project, yet paid from another source, we upgraded the system by placing it on a mobile platform (see Figure 16). This allows the SODAR to be moved almost anywhere and be deployed quickly (within one hour). With the SFAS “as is” a large sound-screen is needed which is very laborious to set-up. For short measurement sessions of less than one day, the system can be ran of batteries. The fact that the SODAR is made mobile and can be deployed anywhere when running for short periods is crucial in the initial deployment at Schiphol. It allows us to do test-runs at numerous locations and so find the optimal spot for the sensor.



Figure 16: SODAR mobile platform developed during this project. The SODAR with small sound-screen is transported inside the trailer and is deployed on the roof of the trailer during an experiment. Processing units and computers are placed inside the trailer.

2.2.3 Experimental set-up

The first test-run of the SODAR was performed in October/November 2011 at the meteorological station the Veenkampen in Wageningen (see Figure 17). The main goal was to test the and get acquainted with the system. The test was satisfactory, no results of this campaign will be shown here.



Figure 17: First field-tests of the mobile SODAR platform in Wageningen (left) and at Cabauw (right).

Next we did a field-test aimed at validating the SODAR against measurements of the Cabauw tower (in The Netherlands), see Figure 17. Data were gathered with the SODAR from the 6th of March 2012 until the end of April 2012. The averaging interval over which the wind speed and wind direction is determined was varied between 2, 5, 10 and 30 minutes. The lower the averaging time the lower the maximum height that can be reached. Therefore, the maximum height was varied between 80 (2 min averaging), 150 (5 min averaging) and 200 m (10 and 30 min averaging). The SODAR took measurements between 7:00 till 19:00 LT to avoid noise pollution for the neighbours during the night. At Cabauw the wind speed and wind direction are measured at 10, 20, 40, 80, 140, and 200 m height. The wind direction is measured at all three booms of the mast, while the wind speed is measured at two booms (North and South-West). At 10 and 20 m height the wind direction and wind speed are measured at two separate masts, North and South of the tower. For each 10 minute interval the instruments are selected where the wind field is least disturbed by the tower itself. Still some flow obstruction remains due to the presence of the tower. Corrections are applied according to Wessels (1983). Corrections in the wind speed are maximal 3% and in wind direction are maximal 3° (Bosveld, 2012). The wind speed is measured at the tower with KNMI cup-anemometer. The cups are calibrated in the wind tunnel of the KNMI. The accuracy of the cup anemometers are 0.5 m s^{-1} , with a threshold velocity of 0.5 m s^{-1} and a resolution of 0.1 m s^{-1} . Wind direction is measured with the KNMI wind vane. The wind vane has an accuracy of 3° and a resolution of 1° (Bosveld, 2012).

2.2.4 Results

We will focus on the results obtained with the 10 minutes averaging interval, with a vertical resolution of 5 m, a maximum measurement height of 200 m, and a tilt angle of 24°. The results for the horizontal wind speed (U) for this set-



up are plotted for different heights in Figure 18; corresponding regression statistics are stated in Table 3.

Table 3: Regression statistics and Root mean square error (RMSE) of the horizontal wind speed of the SODAR with the Cabauw tower and the percentage of SODAR data available (N).

Height [m]	Regression equation	R ² [-]	RMSE [m s ⁻¹]	N [%]
20	$0.93 \cdot U_{tower} - 0.14$	0.60	1.1	94
40	$0.85 \cdot U_{tower} - 0.30$	0.63	0.97	96
80	$1.0 \cdot U_{tower} + 0.076$	0.75	0.99	88
140	$1.0 \cdot U_{tower} + 1.0$	0.72	1.2	44
200	$1.0 \cdot U_{tower} + 1.5$	0.62	1.2	11

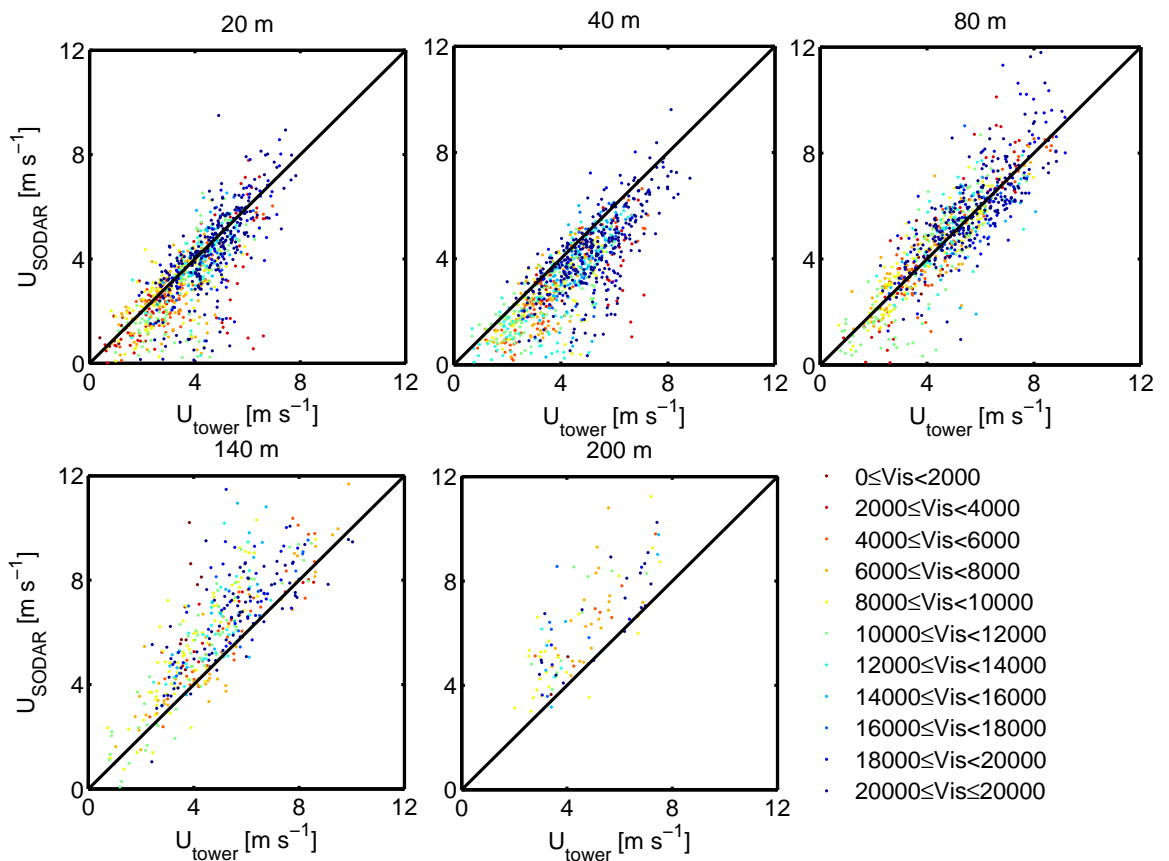


Figure 18: The horizontal wind speed [m s⁻¹] measured at the Cabauw tower against that measured by the SODAR, colour coded with visibility [m] for the 20, 40, 80, 140, and 200 m measurement height.

From Figure 18 and Table 3 it is immediately apparent that less data are available for greater heights. The SFAS64 has a few quality control classes (QC) which are stated in Table 4. The percentage occurrence of these QC-classes at the dif-



ferent heights is given in Table 5. From these Tables it is apparent that at 140 and 200 m a low backscattered signal (QC 0, 1, and 2) is causing the lower amount of data points. The reason that the SODAR is not able to reach this layer is that there are apparently not enough temperature inhomogeneities to backscatter the sound waves or the sound waves are blown away. A SODAR assumes a homogenous wind field across its sampling volume. At 10 m height this homogeneity of the wind field (QC 4 and 5) is in 37% violated, but also a low backscattered signal is a problem. The low signal can be caused by the fact that at low measurement heights the SODAR needs to record the return sound very fast after emitting the sound.

At Schiphol wake vortices can cause a heterogenous wind field, possibly resulting in data loss. At greater height this can result in more data loss due to the higher sampling volume (see Table 6). Therefore, it might be advisable to use the small tilt angle (19°) of the SODAR SFAS64.

Table 4: Description of the quality control classes of the SFAS64

Quality class	Description
0	No data measured or unable to determine data
1	Low cumulative significance and low significance density
2	Low significance density
3	Low cumulative significance
4	Consistency check not applicable because of invalid other wind component
5	Consistency check failed
10	High confident level
11	Very high confident level and all threshold significantly highly exceeded

Table 5: Occurrence [%] of the different quality classes for 10, 20, 40, 80, 140, and 200 m height.

Height [m]	10	20	40	80	140	200
QC						
0	11	0.2	0.1	0.8	12	25
1	27	0	0	0.16	18	37
2	0	0.1	0	6.5	23	21
3	24	0	0	0	0	0
4	23	2.3	1.8	2.4	2.3	2.8
5	14	3.4	2.2	1.1	1.2	3.2
10	0	71	40	68	41	11
11	0	23	56	20	2.8	0



Table 6: Area [m²] of volume scanned by the SFAS64 for a tilt angle of 19° and 24°.

Height [m] Tilt [°]	10	20	40	80	140	200
19	42	159	615	2422	7367	14994
24	69	262	1021	4035	12292	25033

Besides the amount of data loss the SODAR seems to be able to obtain U correctly, especially for the 20 and 80 m height. However, U is underestimated at 40 m height, while it is overestimated at 140 and 200 m heights. Possible cause for the underestimation is fixed echoes, which are site and height depended (Vogt and Thomas, 1995). Another possible cause of the underestimation is overspeeding of the cup anemometers in cases where the wind speed fluctuates. The scatter of U of the SODAR with that of the tower does not seem to increase as the visibility drops.

In Table 7 the percentage of data loss for different visibility classes are given. From the Table we can conclude that most of the data loss is not the result of poor visibility, since the highest percentages of data loss occur when the visibility is 20 km or higher.

Table 7: Percentage of data loss for different visibility classes

Height [m] Class [km]	20	40	80	140	200
0 ≤ vis < 2	0	0	1.6	2.7	2.4
2 ≤ vis < 4	15	4.9	13	11	7.1
4 ≤ vis < 6	5.0	2.4	4.0	4.6	3.3
6 ≤ vis < 8	1.7	0	1.6	6.0	5.3
8 ≤ vis < 10	5.0	2.4	4.0	9.6	9.1
10 ≤ vis < 12	0	2.4	20	13	18
12 ≤ vis < 14	5.0	0	6.5	5.0	7.7
14 ≤ vis < 16	1.7	2.4	1.6	3.2	4.8
16 ≤ vis < 18	0	2.4	5.7	2.9	5.0
18 ≤ vis < 20	12	4.9	6.5	14	10
vis ≥ 20	55	78	34	28	26

A SODAR can also aid airports by detecting the top of the fog layer. A peak in acoustic backscatter is generated by high turbulence activity in the inversion layer associated with the top of a fog layer (Dabas *et al*, 2011). The Royal Netherlands Meteorological Institute (KNMI) already operates a SODAR (a METEK PCS2000-64 SODAR) at Schiphol airport. They investigated the use of the SODAR to determine the top of the fog layer. They found that the SODAR was in-



deed able to give information on the depth of the fog layer (de Haij, 2010). However, the SODAR they use has its lowest measurement height at 50 m. Therefore, it is not suitable to measure the depth of shallow fog layers. The SFAS64 we use has its lowest measurement height at 10 m, making it more suitable to measure the depth of shallow fog layers.

In Figure 19 the wind direction of the SODAR is plotted against that of the tower, colour coded with the horizontal wind speed. The SODAR obtains similar wind directions as the tower. However, when the wind speed is low ($< 3 \text{ m s}^{-1}$) there is more scatter between the wind direction measured by the SODAR and Cabauw tower. This scatter does not necessarily mean that the SODAR measures the wind direction incorrectly, since the wind can whirl more easily when the wind speed is low. Therefore, there can be a difference in wind direction between the air measured by the Cabauw tower and SODAR, which are located approximately 300 m apart.

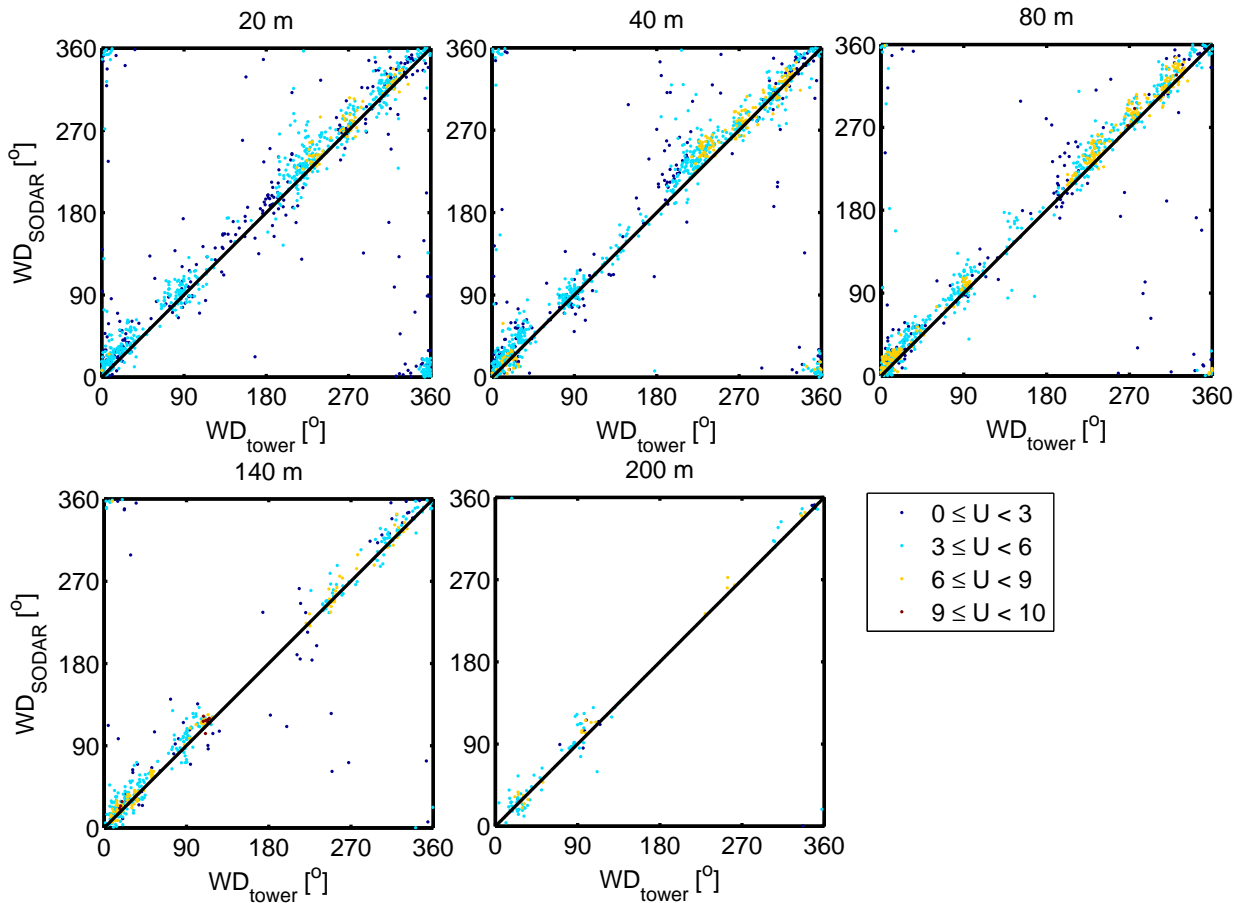


Figure 19: Wind direction at 20, 40, 80, 140, and 200 m height from the Cabauw tower against the SODAR colour coded with the Cabauw tower wind speed, U , [m s^{-1}].



As mentioned before the SODAR was also set-up to measure the wind field at 2 minutes interval, reaching a maximum height of 80 m. First results of this set-up are shown in Figure 20. The results indicate that the SODAR is also able to obtain the wind field for this short interval and at relatively short heights. However, the results of the 2 minute interval still have to be compared to the tower measurements.

35

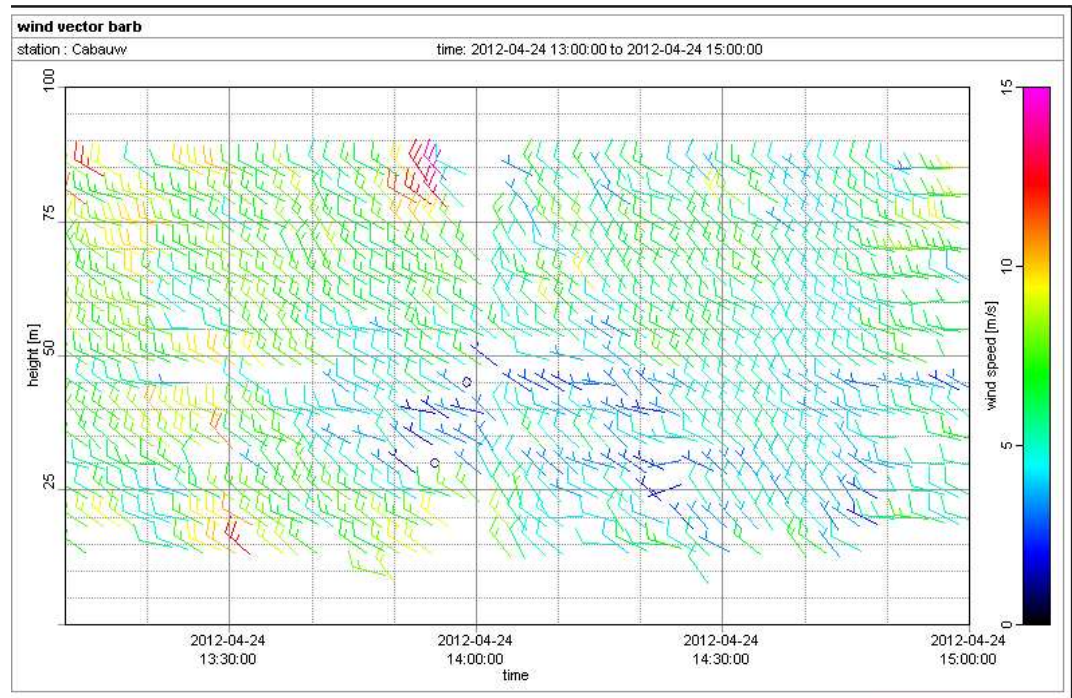


Figure 20: Wind vector measured by the SODAR at 2 minutes interval for 24-04-2012 from 13:00 till 15:00 UTC.

2.2.5 SODAR compared to LIDAR

There are a few studies comparing wind fields measured by a SODAR with that of a LIDAR (e.g. Chintawongvanich et al., 1989 and Bourgeois et al., 2008). Main findings are that the data availability is lower for the SODAR than for the LIDAR. The SODARs used in these studies had difficulty resolving very high windspeeds ($>20 \text{ m s}^{-1}$), since the sound is then dispersed too much to yield a detectable reflection back to the sensor. On the other hand, the SODAR performs better in rainy conditions. For the LIDAR the results for the wind speed and direction in general seems to be agree better with tower measurements, than that of the SODAR. However, this is partly due to the fact that in general the SODAR is placed further away from the tower, since it has problems with backscatter of the tower itself. In all, we think that a LIDAR has some advantages over SODAR for WindVisions, but the results of our SODAR experiment at Cabauw shows



that the SODAR performs well enough to proceed with this instrument in this project.

2.2.6 Conclusions

The SODAR wind field measurements are comparable to that of the tower measurements. However, some measurements height (80 m) have a better agreement with the tower than other levels. In general the horizontal wind speed seems to be overestimated at greater heights (140 and 200 m, with regression off-sets of 1 and 1.5). The wind direction compared very well to that of the tower. However, some scatter occurred in the wind direction measured by the SODAR for low wind speed. For the application for WindVisions this will not cause a problem, since the low wind speeds do not introduce a safety risk for aircrafts landing or taking off.

Using the SODAR for WindVisions there will be a trade-off between the maximum measurement heights and the temporal resolution of the measurements. The higher the temporal resolution the lower the measurement height. However, ideally the wind field measurements have to be directly available for WindVisions. Therefore, a short averaging interval is preferable for the SODAR. First results with a 2 minute interval were shown. However, the 2 minute results still have to be validated against the tower measurements.

In all the SFAS64 SODAR performs well enough to proceed with this instrument as part of WindVisions. Ideally, we would have liked to also include a LIDAR in the Cabauw inter-comparison and future work at Schiphol. Unfortunately we do not have such an instrument available and acquiring one is far beyond the means available in this project (price is between 400 and 500k€).



3 Conclusions and Outlook

The objective of this project is to develop a Wind and Visibility Monitoring System (WindVisions) at airports. The system will consist of a by a horizontal long range wind sensor, a so-called cross-wind scintillometer complemented by a vertically scanning remote sensing instrument, a so-called sound detecting and ranging instrument (SODAR). The area of interest to monitor is the landing and take-off course of airplanes ranging from the surface to about 300m height along a runway

This report describes Phase 1 of WindVisions, which is characterized by the development and testing of the system.

First we developed the WindVisions hardware. A BLS900 scintillometer by Scientc AG, Rottenburg, Germany was purchased and prepared for field work, i.e. processing units, power and signal interfacing and a data logging mini-pc were fitted in rugged field-case. A mobile platform was built for the SODAR already owned by the Meteorology and Air Quality group of Wageningen University. This allows the system to be quickly deployed at virtually any location. The SODAR trailer was not originally planned within the project, but it will be a necessary step for future testing at Schiphol Airport. The funding for this development was independent from this project.

Second we developed the WindVisions methodology. Existing algorithms were improved and new algorithms were developed to obtain the cross-wind from single aperture scintillometers. The results of this work have been submitted to the Journal of Atmospheric and Oceanic Technology. What remains to be done is the development of a visibility algorithm for the scintillometer. We are currently working on this.

Last we tested the WindVisions components at the Haarweg and Veenkampen in Wageningen and at the KNMI observatory at Cabauw. These experiments were aimed at testing the hardware, the algorithms, and the range of applicability. Especially for the SODAR there will be a trade-off between the maximum measurement heights and the temporal resolution of the measurements. The higher the temporal resolution the lower the measurement height.

The results of the methodology development and testing are outlined in the following.

Regarding the cross-wind scintillometer work, we obtained the crosswind from a single aperture scintillometer (SA-LAS) signal using three different algorithms, which are based on scintillation spectra without a calibration in the field. These algorithm are; the corner frequency (CF), maximum frequency (MF) and cumu-



lative spectrum (CS). All three algorithms obtained similar results for the crosswind compared with a sonic anemometer, thereby proving that the three algorithms are able to obtain the crosswind from a scintillometer signal. However, some filters needed to be applied to obtain these results. A filter on the scintillometer intensity signal (I) was applied to all algorithms ($I < 20\ 000$).

From the results we obtained, we conclude that the CS algorithm is best qualified to obtain crosswinds. First, because it is the algorithm with the best fit and lowest scatter with the sonic anemometer. Second, the results of the wavelet spectra also indicated that this method is best suited to obtain the crosswind over 1 second.

For WindVisions the wind measurements ideally have to be available in real time. This can be achieved by using a measurement card which continuously computes FFT spectra. However, for the lower frequencies the longer time-scales will determine the height of the scintillation power spectrum. Therefore, it is advisable to use a SA-LAS algorithm where the salient point in the spectrum is located at higher frequencies. For the CS algorithm this is the case, especially for the 0.9 point in the cumulative spectrum. Future research will therefore focus on obtaining the crosswind real time using the CS algorithm.

Regarding the SODAR work, the experiment at Cabauw revealed that the SODAR wind field measurements are comparable to that of the tower measurements. However, some measurements height (80 m) have a better agreement with the tower than other levels. In general the horizontal wind speed seems to be overestimated at greater heights (140 and 200 m, with regression off-sets of 1 and 1.5). The wind direction compared very well to that of the tower. However, some scatter occurred in the wind direction measured by the SODAR for low wind speed. For the application for WindVisions this will not cause a problem, since the low wind speeds do not introduce a safety risk for aircrafts landing or taking off.

Using the SODAR for WindVisions there will be a trade-off between the maximum measurement heights and the temporal resolution of the measurements. The higher the temporal resolution the lower the measurement height. However, ideally the wind field measurements have to be directly available for WindVisions. Therefore, a short averaging interval is preferable for the SODAR. First results with a 2 minute interval were shown. However, the 2 minute results still have to be validated against the tower measurements.

In all the SFAS64 SODAR performs well enough to proceed with this instrument as part of WindVisions.

One final test we propose to undertake is to set-up the scintillometer with a network of 20 or more wind-speed measurements along the path to clearly identify the difference between the two approaches.



The work in Phase 1 has been performed to a large extent independently from the other partners and stakeholders in the project. They were kept updated through the KvK progress reports (twice a year) and meetings in the framework of the Knowledge Development Centre (KDC), KvK or other settings typically two to three times a year. In Phase 2 we will work more closely together with the other partners and stakeholders as the work will focus more on application of WindVisions at Schiphol.

Phase 2 of WindVisions is geared towards the operational implementation of the system at Schiphol Airport.

The system will then also be embedded in a total package of wind and visibility measurements and forecasts from HARMONIE, a non-hydrostatic meteorological forecast model with a spatial resolution of around 2 km model. The application of HARMONIE at Schiphol is developed as part of the accompanying KvK project IMPACT (Improved Meteo Predictions for Airport Capacity Tuning - HSMS03). The measurements provided by WindVisions and the gained insight on the performance of HARMONIE with respect to the critical weather parameters precipitation and wind is of direct use for hotspot Schiphol Mainport. It should help in their decision process to make optimally use of runway capacity. Also the evaluation of present-day and future severe events may provide guidelines for Schiphol Mainport of how to respond to a future climate.

Looking towards the future, given the vulnerability of Schipol to climate change, building up a consistent long-term dataset monitoring the behaviour of wind and its extremes will be vitally important in assessing the effects of climate change, and will provide societal benefits in the capacity-efficient management of the airport and protection of its economic benefits. The application of sound propagation should not be overlooked since at many airports flight capacity is limited by noise abatement orders and the WindVisions data could play an important role in assessing noise reduction interventions.

The WindVisions datasets will provide an important resource in planning future developments and operation schedules for Schipol, which have both national and international benefits, economic and environmental (e.g. reduction in CO₂ emissions by more efficient runway alignment with the prevailing wind). Ultimately these future plans will have associated multi-billion Euro costs and therefore it is essential that these long-term investments are made with the benefit of the high quality data that WindVisions will provide.

Military applications are also important – both for runway operations and also for toxic plume monitoring and modelling.

In general, this work has in potential a much broader application than airports and transportation, for example in crop irrigation evaporation measurement and monitoring wind speed and air pollution in urban areas. Scintillometers are



now commonly used throughout the world, particularly in China, and these techniques will be applicable to them.

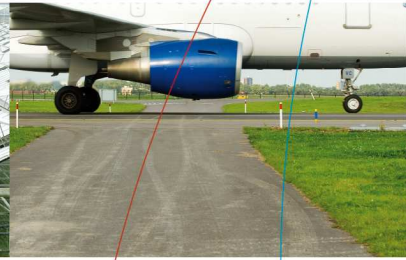
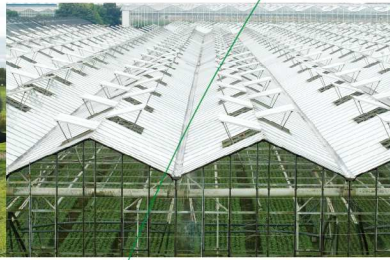


4 Literature

- Beyrich, F., H. A. R. De Bruin, W. M. L. Meijninger, J. W. Schipper, and H. Lohse, 2002: Results from one-year continuous operation of a large aperture scintillometer over a heterogeneous land surface. *Boundary-Layer Meteorology*.
- Bosveld, F.C., 2012. Cabauw observational program on landsurface-atmosphere interaction (2000 - today). <http://www.knmi.nl/~bosveld/experiments/documentation/> (accessed 18-04-2012).
- Bourgeois S., R. Cattin, I. Locker & H. Winkelmeier, 2008. Analysis of the vertical wind profile at a Bura-dominated site in Bosnia based on SODAR and ZEPHIR LIDAR measurements. *Proceedings of European Wind Energy Conference*.
- Chintawongvanich P., R. Olsen & C. A. Biltoft, 1989. Intercomparison of wind measurements from two acoustic Doppler Sodars, a laser Doppler Lidar, and in situ sensors. *Journal of Atmospheric and Oceanic Technology*, **6**, 785–797.
- Clifford, S. F., 1971: Temporal-frequency spectra for a spherical wave propagating through atmospheric turbulence. *Journal of the Optical Society of America*, **61**, 1285–1292.
- Dabas, A., S. Remy, and T. Bergot, 2011: Use of a Sodar to Improve the Forecast of Fogs and Low Clouds on Airports. *Pure and Applied Geophysics*.
- de Haij, M., 2010: *On the use of SODAR reflectivity data during low visibility conditions at Schiphol Airport*, Internal report KNMI, IR2010 – 02.
- Furger, M., P. Drobinski, A. S. H. Prévôt, R. O. Weber, W. K. Graber, and B. Neininger, 2001: Comparison of Horizontal and Vertical Scintillometer Crosswinds during Strong Foehn with Lidar and Aircraft Measurements. *Journal of Atmospheric and Oceanic Technology*, **18**.
- Green, A. E., M. S. Astill, K. J. McAneney, and J. P. Nieveen, 2001: Path-averaged surface fluxes determined from infrared and microwave scintillometers. *Agricultural and Forest Meteorology*, **109**, 233–247.
- KNMI: 2008, De Toestand Van Het Klimaat in Nederland 2008, Royal Dutch Meteorological Institute (KNMI), De Bilt, the Netherlands. Editor: F. Brouwer, 48 pp
- Meijninger, W. M. L., A. E. Green, O. K. Hartogensis, W. Kohsiek, J. C. B. Hoedjes, R. M. Zuurbier, and H. A. R. De Bruin, 2002a: Determination of area-averaged water vapour fluxes with Large Aperture and Radio Wave Scintillometers over a heterogeneous surface—Flevoland Field Experiment. *Boundary-Layer Meteorology*, **105**, 63–83.
- Meijninger, W. M. L., O. K. Hartogensis, W. Kohsiek, J. C. B. Hoedjes, R. M. Zuurbier, and H. A. R. De Bruin, 2002b: Determination of area-averaged sensible heat fluxes with a large aperture scintillometer over a heterogeneous surface—flevoland field experiment. *Boundary-Layer Meteorology*, **105**, 37–62.



- Nieveen, J. P., A. E. Green, and W. Kohsiek, 1998: Using a large-aperture scintillometer to measure absorption and refractive index fluctuations. *Boundary-Layer Meteorology*, **87**, 101–116.
- Oncley, S. P., C. A. Friehe, J. C. Larue, J. A. Businger, E. C. Itsweire, and S. S. Chang, 1996: Surface-layer fluxes, profiles, and turbulence measurements over uniform terrain under near-neutral conditions. *Journal of the Atmospheric Sciences*, **53**, 1029–1044.
- Poggio, L. P., M. Furger, A. H. Prévôt, W. K. Graber, and E. L. Andreas, 2000: Scintillometer Wind Measurements over Complex Terrain. *Journal of Atmospheric and Oceanic Technology*, **17**, 17–26.
- Van Dinther, Danielle, Hartogensis, Oscar K. and Arnold F. Moene, 2012: Crosswind from a Single Aperture Scintillometer using Spectral Techniques. *submitted to Journal of Atmospheric and Oceanic Technology*.
- Vogt, S., and P. Thomas, 1995: SODAR — A useful remote sounder to measure wind and turbulence. *Journal of Wind Engineering and Industrial Aerodynamics*, 54-55, 163–172.
- Ward, H. C., J. G. Evans, and C. S. B. Grimmond, 2011: Effects of Non-Uniform Crosswind Fields on Scintillometry Measurements. *Boundary-Layer Meteorology*.
- Wessels, H. R. A., 1983. *Distortion of the Wind Field by the Cabauw Meteorological Tower*, Internal report KNMI, 83-15.
- Wilczak, J. M., S. P. Oncley, and S. A. Stage, 2001: Sonic anemometer tilt correction algorithms. *Boundary-Layer Meteorology*, **99**, 127–150.
- Wong, D. K. Y., D. E. Pitfield, R. E. Caves, and A. J. Appleyard, 2006: Quantifying and characterising aviation accident risk factors. *Journal of Air Transport Management*, **12**, 352–357.



To develop the scientific and applied knowledge required for
Climate-proofing the Netherlands and to create a sustainable
Knowledge infrastructure for managing climate change

Contact information

Knowledge for Climate Programme Office

Secretariat:

c/o Utrecht University

P.O. Box 80115

3508 TC Utrecht

The Netherlands

T +31 88 335 7881

E office@kennisvoorklimaat.nl

Public Relations:

c/o Alterra (Wageningen UR)

P.O. Box 47

6700 AA Wageningen

The Netherlands

T +31 317 48 6540

E info@kennisvoorklimaat.nl

www.knowledgeforclimate.org

